Power Management of Intelligent Buildings Facilitated by Smart Grid: A Market Approach

Quang Duy La, *Member, IEEE*, Yiu Wing Edwin Chan, *Student Member, IEEE*,
and Boon-Hee Soong, *Senior Member, IEEE*

Abstract—The emergence of smart grid technology is offering a unique opportunity to improve power management in intelligent buildings through the integration and optimization of distributed energy resources and loads. In this paper, the interactions of multiple intelligent buildings in the context of energy market, as well as distributed energy generation and storage facilities, is considered. Within a time horizon divided into multiple periods in which generations and loads are forecasted, each building in a certain period may experience power surplus or deficit. While any deficit can be obtained from the market, buildings may consider selling their unused power back to the market. A dynamic pricing model based on differential game theory is set up in order to study the interactions of these players and how they maximize their profit. We also propose algorithms to implement and operate the system over the time horizon considered. Furthermore, numerical studies are performed to validate the model and algorithms.

Index Terms—Distributed energy resources (DER), energy market, game theory, intelligent buildings, smart grid.

NOMENCLATURE

α, β	Cost coefficients in player's utility function.
γ	Price adjustment coefficient in buyer market.
ϵ	Storage capacity loss coefficient.
η	Storage charge/discharge efficiency.
η_{PV}	Solar conversion efficiency.
$\pi(t)$	Instantaneous price of seller market, \$/kW.
Π_0, π_0	Initial prices, \$/kW.
Π_n	Price of buyer market in the interval n, \$/kW.
a, k, λ	Price trajectory coefficients in seller market.
$h, h_{\max}$	Actual and maximum stepsizes.
i, j	Indices of buildings/players.
n	Index of time steps or intervals.
r	Discount rate in player's utility function.

t	Instantaneous time.
t_n	Sequence of time steps.
$v_i(t)$	Wind speed at building i, m/s.
$v_{\mathrm{in}}, v_{\mathrm{out}}, v_r$	Cut-in, cut-out, and rated wind speeds for wind turbine, m/s.
A_{PV}	Area of photovoltaic (PV) cells, m^2.
C_0	Initial capacity of storage device, kWh.
$C_i^s(t)$	Capacity of storage device of building i, kWh.
E_i^g, E_i^l	Generation and load energy forecasts of building i, kWh.
E_i^m	Available energy for trading of building i, kWh.
$E_i^s(t)$	Instantaneous storage energy of building i, kWh.
$I_{\mathrm{PV},i}(t)$	Solar irradiance at building i, kW/m^2.
J^*, J_d	Theoretical and discrete-time total profits, \$.
J_i	Accumulated utility function of building i, \$.
M	Number of buildings in the cluster.
N	Number of buildings with power surplus.
$P_i^g(t)$	Generator output power of building i, kW.
$P_i^l(t)$	Load consumption power of building i, kW.
$P_i^m(t)$	Instantaneous market-traded power of building i, kW.
P_i^{m*}	Optimal strategy for building i, kW.
$P_{-i}^m(t)$	Joint strategies of buildings other than i.
$P_i^s(t)$	Effective storage charge/discharge power of building i, kW.
$P_i^{s\dagger}(t)$	Actual storage charge/discharge power of building i, kW.
$P_{\max}^s$	Maximum charge rate of storage device, kW.
$-P_{\min}^s$	Maximum discharge rate of storage device, kW.
P_{WT}	Rated wind turbine power, kW.
$\widetilde{P}_i^g, \widetilde{P}_i^l$	Forecasts of generator and load power of building i, kW.
$\widetilde{P}_i^m$	Available power for trading of building i over the interval, kW.
$\widetilde{P}_i^s$	Average output power of storage device of building i over the interval, kW.
$\widehat{P^m}$	Common effective power constraint, kW.
Q_n	Total power demand in buyer market for interval n, kW.
T	Duration of intervals, minutes.
T_{air}	Outside air temperature, °C.
$V(\pi)$	Differential game's value function.

I. INTRODUCTION

BUILDINGS, as an integral part of modern human society, is one major energy consumer. For instance, 31% of Singapore's electricity generation in 2005 [1] and about 35% of USA electricity consumption in 2010 [2] were attributed to nonresidential or commercial buildings. The figures are expected to rise given the current rate of world population growth and urbanization. In order to better manage the energy demand and increase the building energy efficiency, an intelligent building often employs a building automation system (BAS) to monitor and optimally control various building loads such as lighting and heating, ventilating, and air conditioning (HVAC) systems.

The recent development of smart grid technology offers a unique opportunity for intelligent buildings to actively manage their power. First, modern information and communications technology allows two-way communications between electricity suppliers and consumers, and facilitates demand response (DR). Another major benefit is the incorporation of distributed energy resources (DERs), including distributed generation (DG) and distributed storage (DS). DG units, usually small-scale on-site energy generators, bring the point of generation closer to loads, hence reducing transmission loss and enhancing the voltage profile [3]. Due to increasing fuel cost and growing environmental concern, renewable energy sources, such as PV panels and wind turbines, are quickly becoming popular alternatives to traditional fossil-fuel generators. As renewable energy is, however, fluctuating and intermittent in nature, DS devices can be deployed to smoothen the variations. In addition, they can discharge and augment the generation when the load peaks, or store any unused energy. Several forms of DS are common, ranging from batteries, supercapacitors to flywheels [4]. Fig. 1 shows the aforementioned components in one intelligent building, which in turn is part of a building cluster interconnected by smart grid. This allows the buildings to actively interact with each other as well as the utility companies in the energy market.

A. Related Works

In the literature, several works have addressed the integration and operation of DERs in smart grid. In order to match the power generation and demand in an islanded microgrid, Marzband *et al.* [5] used single side auction mechanism to determine the market clearing price. The use of distribution locational marginal price as the pricing signal to control a power distribution system with DG and DS is described in [6]. In the EcoGrid EU real-time market [7], the system operator settles the price in a huge optimization problem requiring vast information such as device capacities and consumers' and DERs' responses. Nguyen and Le [8] proposed a stochastic program to control the generation, storage and energy scheduling and bidding in response to the market price, in order to maximize the expected benefit of community-scale microgrid. Ding *et al.* [9] formulated a single wind turbine profit maximization problem where wind energy either serves associated loads or is sold on a green energy market. However, they do not consider energy storage or interaction between multiple
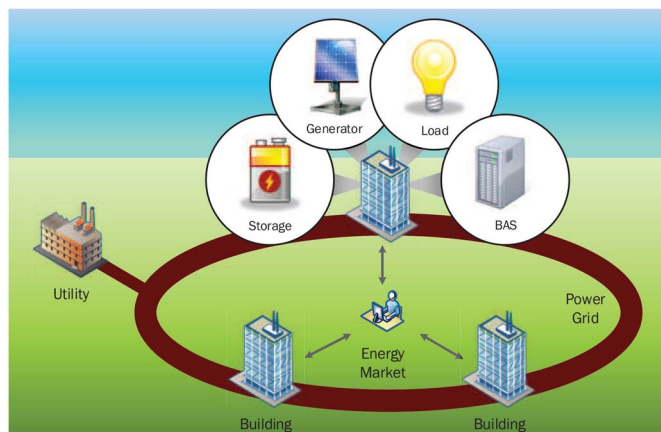

Fig. 1. System model.

systems. Damiano *et al.* [10] studied scheduling and real-time control of energy storage system in order to maximize renewable energy usage. Despite a similar setting to ours, multiple units and selling of energy are not considered. Lee *et al.* [11] discussed the macroeconomic benefits of enabling direct trading between small-scale energy suppliers and end users by forming one grand coalition and determining the direct-trading price and revenue distribution. This paper, however, does not address the benefit for individual players.

Addressing the operation of an intelligent building facilitated by smart grid, Guan *et al.* [12] solved the scheduling problem of energy source and load in order to minimize total energy cost. In a scenario where the building owner provides energy to tenants at variable price, energy consumption is managed via incentive pricing in [13]. A mathematical framework for DR for commercial building with generation and storage elements is presented in [27]. In [28], an optimization framework is presented to handle DR and manage DER such that a community of smart homes can benefit by lowering the overall energy consumption. Lee *et al.* [29] studied the joint scheduling problem of energy supply and demand for homes and buildings to minimize the energy cost under some known tariffs. Optimizing the energy management in a single DER-equipped building is considered in [30], where uncertainties in load demand and renewable energy generation are captured via chance constrained two-stage stochastic programming. GreenCharge [31] is proposed to manage renewable energy generation, storage, and grid energy in a building in order to minimized the cost for buying electricity from the grid. Most of the aforementioned works, however, are from the perspective of a single building. In the smart grid literature (see [14] and references therein), research works for multiple buildings within a cluster in an energy market context are still relatively few.

B. Our Contributions

To address the lack of works on intelligent buildings facilitated by smart grid, in this paper, we build upon our previous work's model [15] while considering the operation of DERs in intelligent buildings, and how a building manages its power flow so as to maximize its own benefit, in the presence of other buildings' simultaneous actions which may cause conflict of

This article has been accepted for inclusion in a future issue of this journal. Content is final as presented, with the exception of pagination.

LA *et al.*: POWER MANAGEMENT OF INTELLIGENT BUILDINGS FACILITATED BY SMART GRID: A MARKET APPROACH

3

interest. While a building is serving its own loads, any energy surplus can be either stored or sold to the market; at the same time, any deficit can be sourced from the market.

In [15], the pricing mechanism uses energy as a unit good to be priced and traded. It is noticed that by nature, energy is some quantity spanning a period of time, thereby rendering it unsuitable for a dynamic pricing model where the commodity is traded and price-adjusted continuously over time. Instead, we price power dynamically, which is appropriate as power is itself the rate of energy flow. Furthermore, the consideration of power allows us to address the storage device constraints.

The main contributions of this paper are threefold as follows.

1) Assuming real-time power pricing, we develop a generic model for intelligent buildings with the basic components of generator, storage, and loads. While addressing their inherent constraints, the model also allows two-way energy trading via a broker.

2) For the seller market formulated as an oligopoly differential game, we give the theoretical solution to the dynamic price and players' optimal strategies at equilibrium.

3) We present an implementation algorithm that invokes a discrete-time price and strategy update scheme, which approximates the ideal theoretical results. The convergence condition of this scheme is fully characterized.

II. SYSTEM MODEL

We aim to manage power usage of intelligent buildings in a cluster over a given time horizon. For clarity, we assume each building has one aggregate generator, storage, and load. There are M such buildings in the cluster. Next, we describe a generic model for the ith building.

A. Generic Model of Buildings

The BAS in each building coordinates its generator, storage and load, as illustrated in Fig. 1, and interfaces with the energy market. The M buildings interact with each other as well as the market and are considered players in a game-theoretic model.

1) Generator: We denote the instantaneous output power of the building i's generator as $P_i^g(t)$, where $P_i^g(t) \geq 0$. In this paper, we consider renewable energy generation from solar PV cells or wind turbines.

In the case of solar PV generation, following Chen *et al.* [35], $P_i^g(t)$ is calculated from:

$$P_i^g(t) = \eta_{\text{PV}} A_{\text{PV}} I_{\text{PV},i}(t)(1 - 0.005(T_{\text{air}} - 25)) \tag{1}$$

where η_{PV} is the solar conversion efficiency of PV cells; A_{PV} is the area of PV cells (m^2); T_{air} is the outside air temperature (°C); and $I_{\text{PV},i}(t)$ is the solar irradiance (kW/m^2) at building i.

In the case of wind turbines, based on [35], we have

$$P_i^g(t) = \begin{cases} P_{\text{WT}} \dfrac{v_i(t) - v_{\text{in}}}{v_r - v_{\text{in}}} & v_i(t) \in [v_{\text{in}}, v_r) \\ P_{\text{WT}} & v_i(t) \in [v_r, v_{\text{out}}] \\ 0 & \text{otherwise} \end{cases} \tag{2}$$

where $v_i(t)$ (m/s) is the current wind speed at building i; $v_{\text{in}}, v_{\text{out}}, v_r$ (m/s) are the cut-in, cut-out, and rated wind speeds, respectively; and P_{WT} (kW) is the rated wind turbine power.

2) Load: Building i's local load has an instantaneous power consumption given by $P_i^l(t) \geq 0$. Following similar assumptions of [9] and [16], we only specify that it is a piecewise constant function. Typical load profiles of residential and office buildings with electrical appliances such as air conditioners and lighting follow this characteristic [16].

3) Storage: Following [16], we also assume that there is energy conversion loss during the storage charge/discharge process. Let building i's effective storage charge/discharge power (i.e., as seen at the system's bus) be denoted by $P_i^s(t)$. We distinguish $P_i^s(t)$ from $P_i^{s\dagger}(t)$, the actual storage charge/ discharge power seen at the battery. A constant conversion efficiency coefficient $0 < \eta \leq 1$ is assumed for both charging and discharging [16]. Hence, $P_i^s(t)$ is related to $P_i^{s\dagger}(t)$ by

$$P_i^{s\dagger}(t) = \eta^{s_i(t)} P_i^s(t) \tag{3}$$

where $s_i(t)$ denotes the state of player i's storage device over time, which is 1 when charging and -1 when discharging.

For $P_i^s(t)$, we also adopt the following convention.
1) $P_i^s(t) > 0$ when charging.
2) $P_i^s(t) < 0$ when discharging.

Meanwhile, $P_i^{s\dagger}(t)$ is bounded by the storage device's maximum charge and discharge rate, i.e., $P_{\text{min}}^s \leq P_i^{s\dagger}(t) \leq P_{\text{max}}^s$. We further assume $-P_{\text{min}}^s = P_{\text{max}}^s$. Furthermore, $P_i^{s\dagger}(t)$ is related to the current stored electrical energy $E_i^s(t)$ by $dE_i^s(t)/dt = P_i^{s\dagger}(t)$. Clearly, $E_i^s(t)$ is bounded by the storage capacity $C_i^s(t)$, i.e., $0 \leq E_i^s(t) \leq C_i^s(t)$.

Here, $C_i^s(t)$ is defined as a function of time in order to take into account the effect of storage device aging. The aging model follows that of [16], that is:

$$C_i^s(t) = C_0 - \Delta C_i^s(t) \tag{4}$$

where C_0 is the initial capacity at $t = 0$ (assuming identical among the storage devices of all buildings); and $\Delta C_i^s(t)$ is the accumulated capacity loss at time t and is defined such that

$$\frac{d\Delta C_i^s(t)}{dt} = \begin{cases} -\epsilon P_i^{s\dagger}(t) & \text{if } P_i^{s\dagger}(t) < 0 \\ 0 & \text{Otherwise} \end{cases} \tag{5}$$

where $\epsilon > 0$ is a battery-type-dependent constant. It is implied that capacity is lost only during battery discharging.

B. Energy Market

A building can either sell its excessive power to the market in case of surplus, or buy more power from the market when in shortage. The said energy market can be thought of as a common platform implemented at a centralized controller, who also provides brokering functionality (see Fig. 2). The broker executes several necessary market operations, such as player coordination, price announcement, and price update. As Fig. 2 suggests, the basic market interactions are that a building requests a desired amount of power at the broker, who in turn offers that at a certain price. For building i, $P_i^m(t)$ denotes the amount of traded power, with the following convention.
1) $P_i^m(t) > 0$ when selling to market.
2) $P_i^m(t) < 0$ when buying from market.

This article has been accepted for inclusion in a future issue of this journal. Content is final as presented, with the exception of pagination.
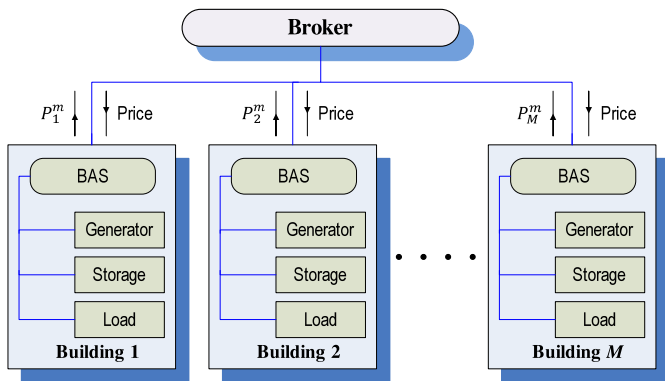
4

IEEE TRANSACTIONS ON SMART GRID

Fig. 2. Energy market model with multiple buildings and a centralized broker.

The mechanism for determining the price Π in the buyer market and π in the seller market will be discussed in detail in Sections III and IV, respectively.

C. Balance Equations and Related Assumptions

For each building, its generator, load, and effective storage powers, as well as power traded with the market are always balanced. That is, at time t, the following balance equation holds:

$$P_i^g(t) = P_i^s(t) + P_i^l(t) + P_i^m(t). \tag{6}$$

1) Assumption: Due to the intermittent nature of renewable energy sources, energy generation forecast has to be done within short timeframes to achieve reasonable accuracy [17]. Hence, we divide the horizon into periods of T time units each. For example, PV power output and load can be assumed constant and predictable in each 30-min period [18]. On the other hand, for wind turbines, a shorter interval of 5 min [9] may be applied due to greater fluctuation. We will therefore assume that forecast for the renewable generation building i during $[0, T]$ are known in terms of the solar irradiance or wind speed. That is, for building i with PV generation, we can assume that $I_{\text{PV},i}(t) = \widetilde{I}_i$; and for wind turbine generation, $v_i(t) = \widetilde{v}_i$ during $t \in [0, T]$. Equivalently, we can write $P_i^g(t) = \widetilde{P}_i^g$, where $\widetilde{P}_i^g$ is a known forecast of building i's generation during $t \in [0, T]$.

Similarly, the load consumption forecast is also known ahead of the period. Thus, $P_i^l(t) = \widetilde{P}_i^l$ for $t \in [0, T]$, where $\widetilde{P}_i^l$ is a constant.

2) Available Power for Trading: At $t = 0$, building i determines its available power for trading and take subsequent actions. We hence define a new variable $\widetilde{P}_i^s$ as the average power output if the storage unit is to fully discharge at a constant rate over the whole period $[0, T]$. If, at time $t = 0$, the available electrical energy in the storage is $E_i^s(0)$, then $\widetilde{P}_i^s \triangleq -\eta E_i^s(0)/T$. Based on the power balance equation (6) and the above assumptions, we obtain the following:

$$\widetilde{P}_i^m = \widetilde{P}_i^g - \widetilde{P}_i^s - \widetilde{P}_i^l \tag{7}$$

where $\widetilde{P}_i^m$ represents the current amount of available power for trading from building i at $t = 0$. Two scenarios can occur as follows.

1) If $\widetilde{P}_i^m > 0$, building i has a maximum power surplus of $\widetilde{P}_i^m$ which can be sold to the market. The actual power sold thus satisfies $0 \leq P_i^m(t) \leq \widetilde{P}_i^m$.
2) If $\widetilde{P}_i^m \leq 0$, building i has a power deficit. The amount lacking will be purchased from the market.

Alternatively, (7) can be re-expressed into

$$E_i^m = E_i^g + E_i^s(0) - E_i^l$$

where E_i^g, E_i^l are the known forecasts of energy generation and load consumption over $[0, T]$, and $E_i^s(0)$ is the available energy in the storage device at $t = 0$. When player i is in surplus, E_i^m is the maximum amount of energy player i can trade to the market during $[0, T]$. Thus, $\widetilde{P}_i^m$ gives an upper bound on $P_i^m(t)$. If $P_i^m(t) > \widetilde{P}_i^m$, it may occur that $\int_0^T P_i^m(t)dt > \widetilde{P}_i^m T = E_i^m$ which is not allowable since the total energy sold is upper-bounded by E_i^m. A rationale for using $\widetilde{P}_i^m$ is that, while theoretically $P_i^m(t) > \widetilde{P}_i^m$ might be possible during some fraction of the time, one would like to avoid undesirable effects to the battery such as lifetime reduction which can be caused by discharging the battery at high power.

During the market participation, the actual amount $P_i^m(t)$ at time t varies dynamically; and so do $P_i^s(t)$ and $P_i^{s\dagger}(t)$ in response to $P_i^m(t)$, while at any time its own constraint $P_{\min}^s \leq P_i^{s\dagger}(t) \leq P_{\max}^s$ should also be satisfied. Thus, one can derive $P_i^s(t)$ as

$$P_i^s(t) = \begin{cases} P_i^{s,\text{id}} = \widetilde{P}_i^g - \widetilde{P}_i^l - P_i^m(t), & P_i^{s,\text{id}} \in [\eta P_{\min}^s, \frac{P_{\max}^s}{\eta}] \\ \dfrac{P_{\max}^s}{\eta}, & P_i^{s,\text{id}} > \dfrac{P_{\max}^s}{\eta} \\ \eta P_{\min}^s, & P_i^{s,\text{id}} < \eta P_{\min}^s \end{cases} \tag{8}$$

where $P_i^{s,\text{id}}$ is the ideal effective charging/discharging power under no constraint. When its boundary capacity is reached, this ideal power is not attained and some power has been lost.[1]

D. Market Approach in Case of Power Surplus and Deficit

Without loss of generality, we assume that during the period, there are $N \, (< M)$ buildings in surplus, while the rest are in deficit. For the $M - N$ players with power deficit, they simply purchase the required amount of power in the market for buyers. In Section III, we address the pricing issues in the buyer market. Next, the N players with power surplus enter a market for sellers (assumed separated from the aforementioned buyer market) and compete among each other as the N oligopolists (i.e., sellers in a market dominated by a small number of firms). Then, similar to [15], we can use a differential game framework to establish a dynamic pricing model and then analyze the players' optimal strategies, as well as the price dynamics and the steady-state equilibrium outcomes. The differential game is played over this period $[0, T]$. In Section IV, an analysis of the game will be presented.

---

[1]Subsequently, (6) can be modified to represent this loss by replacing $P_i^s(t)$ by $P_i^s(t) + L_i$, where $L_i = 0$ if $P_i^s(t) = P_i^{s,\text{id}}$.

This article has been accepted for inclusion in a future issue of this journal. Content is final as presented, with the exception of pagination.

LA *et al.*: POWER MANAGEMENT OF INTELLIGENT BUILDINGS FACILITATED BY SMART GRID: A MARKET APPROACH 5

At $t = T$, for player i, a certain amount of energy will have been charged into or discharged from the storage devices, given by $\Delta E_i^s(T) = \int_0^T P_i^{s\dagger}(\tau)d\tau$. Thus, the starting energy amount in the system's storage for the next period $E_i^s(T)$ is

$$E_i^s(T) = \min\{C_i^s(T), E_i^s(0) + \Delta E_i^s(T)\}. \quad (9)$$

That is, any energy surplus that happens to exceed the capacity of the storage will be considered lost.

III. Pricing in the Buyer Market

In the buyer market, buildings with power deficit must buy the exact amount from the backbone grid to replenish their stock; and the broker can handle these transactions. Here, we draw a comparison with the Singapore energy market, where the broker plays the role of a retailer who has previously purchased energy in bulk from the utility company and sells to the "contestable consumers" (the buildings in our case) at its own price [19]. Thus, effectively this market is a monopoly and price is set by the broker.

We propose a dynamic pricing scheme that enables the broker to adjust its price according to the demands of the players. Consider building i with a deficit $\widetilde{P_i^m} < 0$, i.e., $-\widetilde{P_i^m}$ is its demand. The total market demand is $Q = -\sum_{i \notin \mathcal{N}} \widetilde{P_i^m}$. As the system cycles through multiple intervals of duration T, let Π_n be the price in the nth interval. We propose that Π_n be constant during the interval and only change at the start of the next one. The new price Π_{n+1} is

$$\Pi_{n+1} = \Pi_n\left(1 + \gamma \frac{Q_{n+1} - Q_n}{Q_n}\right) \quad (10)$$

where Q_n, Q_{n+1} are the total demands in the corresponding intervals; and γ is an adjustment coefficient. Also, initial price Π_0 equals the current macro-level market price. Our scheme implies that price change is directly proportional to the proportion of demand change $\Delta Q/Q = (Q_{n+1} - Q_n)/Q_n$. In fact, $(1/\gamma) = (\Delta Q/Q)/(\Delta\Pi/\Pi)$ (where $\Delta\Pi/\Pi = (\Pi_{n+1} - \Pi_n)/\Pi_n$) is by definition the price elasticity of demand, an economic measure of the sensitivity of demand to the movement of price. Hence, its inverse γ represents the responsiveness of price due to changing demand. When $\Delta Q/Q > 0$ and $\gamma > 0$, more demands implies a market growth and thus leads to price increase. One rationale for the broker to increase the price here is that due to it prepurchasing energy in bulk, a higher total deficit Q increases the chance of exhausting the broker's quota. When this happens, the broker may have to buy from the real-time market, usually at a higher price, giving it an incentive to charge more to cover its cost. On the contrary, price will decrease when the market is in decline.

IV. Seller Market as Dynamic Oligopoly

A. Game Formulation

We formulate the oligopoly game for the N sellers. Denote $\mathcal{N}$ the set of N buildings in surplus during $t \in [0, T]$. Each player $i \in \mathcal{N}$'s action is to dynamically determine $P_i^m(t)$, the power sold (or output) to the market. We denote $\pi(t) \in \mathbb{R}$ the power price. Note that negative price can be allowed [20]. Similar to various prior studies of electricity market [25], [26], [36], [37], we adopt for our model a standard inverse demand function of Cournot oligopoly as

$$\hat{\pi}(t) = a - \lambda \sum_{i=1}^N P_i^m(t) \quad (11)$$

where $\hat{\pi}(t)$ is called the desirable price level, i.e., price that meets the current total supplies given by $\sum_{i=1}^N P_i^m(t)$. Coefficients $a, \lambda > 0$ are the intercept and slope of the inverse demand curve, respectively. Additionally, we assume that $\lambda < 2N$ so as to ensure market stability, as will be shown later. They are set by the market to control price movement in response to the supplied $\sum_{i=1}^N P_i^m(t)$.

Hence, the dynamics of the market price is such that $\pi(t)$ reacts to the difference between itself and the desirable price level $\Delta\pi(t) = \hat{\pi}(t) - \pi(t)$ according to $\dot{\pi}(t) = d\pi(t)/dt = G(\Delta\pi(t))$. Following [15], we let $G(.)$ be a linear function in $\Delta\pi(t)$, i.e., $G(\Delta\pi(t)) = k\Delta\pi(t)$. As such, the price $\pi(t)$ evolves under the dynamic

$$\dot{\pi}(t) = k\left[a - \lambda \sum_{i=1}^N P_i^m(t) - \pi(t)\right], \quad \pi(0) = \pi_0. \quad (12)$$

Equation (12) is a differential equation in $\pi(t)$, also called the price trajectory. Here, $\pi(0)$ is the initial price at $t = 0$. Player i then adapts its strategy $P_i^m(t)$ according to the current $\pi(t)$ in order to maximize its payoff in the whole period. This objective is represented by the following utility function [15]:

$$J_i(\pi, P_i^m, P_{-i}^m)$$
$$= \int_0^T e^{-rt}\left\{P_i^m(t)\pi(t) - \alpha P_i^m(t) - \beta[P_i^m(t)]^2\right\}dt. \quad (13)$$

Here, P_{-i}^m denotes the joint strategies of player i's opponents, e^{-rt} is a standard discount factor and $r > 0$ the discount rate. $P_i^m(t)\pi(t)$ gives the instantaneous revenue (money) gained from selling $P_i^m(t)$ units of power. $\alpha P_i^m(t)$ accounts for miscellaneous cost, including a commission fee to the broker proportional to the amount of power sold; while $\beta[P_i^m(t)]^2$ is a second-order penalty to prevent the player from selling too much power, resulting in excessive battery discharging and reduced storage lifetime. $\alpha, \beta > 0$ are cost coefficients. The oligopoly differential game can therefore be stated as the following optimization, for each player i:

$$\max_{P_i^m} J_i(\pi, P_i^m, P_{-i}^m)$$
$$\text{s.t.} \begin{cases} \dot{\pi}(t) = k\left[a - \lambda \sum_{j=1}^N P_j^m(t) - \pi(t)\right], & \pi(0) = \pi_0 \\ 0 \le P_i^m(t) \le \widetilde{P_i^m} \ \forall t. \end{cases} \quad (14)$$

The formulated game can be categorized as a linear quadratic differential game, an important class within differential game theory as well as optimal control theory [21]. Applications of linear-quadratic models have been studied for electricity market (see [25], [26]). We also remark that in (12), it is implied that the buildings are price-makers while broker is price-taker. In doing so, we can focus more on the buildings as the key players in the system while the broker assumes the role of a facilitator. Similar assumption can also be found in the literature. For instance, a price-maker model to optimize a wind power producers profit is presented and studied

in [32]. Moreover, price-taking buyers which is an underlying principle of Cournot oligopoly are justified provided that the traded goods from any seller are homogeneous such that the buyers have no incentives to differentiate among individual sellers. Here the broker usually has uniform preference for power sold by all individual buildings and hence it behaves as price-taker.

B. Solution of the General Oligopoly

Before characterizing the game's solution, we first remark that if the time needed for the price and players' strategies to converge to steady-state values is relatively smaller than the duration T, an infinite horizon $T \to \infty$ can be assumed. This assumption will be numerically verified in a subsequent section. As a result, we look for the feedback Nash equilibrium (NE) where each player employs its stationary Markov strategies. These concepts are defined as follows [21], [22].

Definition 1: The strategy function P_i^m of player i can be classified as stationary Markov if $P_i^m \equiv P_i^m(\pi(t))$, which is solely a function of the current state $\pi(t)$.

Definition 2: Consider the game (14) with $T \to \infty$, where all players' strategies are of the stationary Markov type. Then, $(P_1^{m*}, P_2^{m*}, \ldots, P_N^{m*})$ is a stationary feedback Markov NE if for any player i, any $\pi(t)$ at any time t

$$J_i\left(\pi, P_i^{m*}, P_{-i}^{m*}\right) \geq J_i\left(\pi, P_i^{m'}, P_{-i}^{m*}\right), \ \forall P_i^{m'} \not\equiv P_i^{m*}. \quad (15)$$

Using known results from differential game theory, the feedback Markov NE for the game can be characterized by solving the Hamilton–Jacobi–Bellman (HJB) equations [22].

Theorem 1: The differential game (14) with $T \to \infty$ admits a stationary Markov strategy profile $(P_1^{m*}, P_2^{m*}, \ldots, P_N^{m*})$, $P_i^{m*} \equiv P_i^{m*}(\pi)^2$ as a stationary Markov feedback NE if for any player i, there exists a continuously differentiable function $V_i(\pi) : \mathbb{R} \mapsto \mathbb{R}$ that satisfies

$$rV_i(\pi) = \max_{P_i^m} \left\{ \left[\pi P_i^m - \alpha P_i^m - \beta\left(P_i^m\right)^2 \right] + \frac{\partial V_i(\pi)}{\partial \pi} \right.$$
$$\left. \cdot k\left[a - \lambda P_i^m - \lambda \sum_{j=1, j\neq i}^{N} P_j^{m*} - \pi \right] \right\}. \quad (16)$$

Equation (16) are N partial differential equations (PDE), whose solutions are the N functions $V_i(\pi)$, $i = 1, \ldots, N$, commonly known as the value functions. As the maximand in (16) is quadratic in P_i^m, one can carry out the maximization by taking the (partial) derivative of the maximand with respect to P_i^m. We denote this derivative by Φ_i, where

$$\Phi_i = \pi - \alpha - 2\beta P_i^m - k\lambda \frac{\partial V_i}{\partial \pi}. \quad (17)$$

Due to the power constraint $0 \leq P_i^m \leq \widetilde{P_i^m}$, the solution to $\Phi_i(P_i^m) = 0$ will be the optimal strategy P_i^{m*} only when this constraint is satisfied; otherwise the optimal point should occur at the boundaries, i.e., either at 0 or $\widetilde{P_i^m}$, conditioned on the sign of Φ_i. In general, at equilibrium, if there are $K < N$

players whose optimal strategies are either 0 or $\widetilde{P_i^m}$, then for the remaining players, the problem becomes an unconstrained $(N - K)$-player linear-quadratic differential game model [21], in which the corresponding value function of a player i, if exists, takes the quadratic form $V_i = (1/2)X_i\pi^2 - Y_i\pi + Z_i$. Thus, P_i^{m*} can be obtained by substituting $(\partial V_i/\partial \pi) = X_i\pi - Y_i$ in (17) and solving $\Phi_i(P_i^m) = 0$. In summary

$$P_i^{m*} = \begin{cases} \frac{1}{2\beta}[(1 - k\lambda X_i)\pi + (k\lambda Y_i - \alpha)] & \Phi_i = 0 \\ 0 & \Phi_i < 0 \\ \widetilde{P_i^m} & \Phi_i > 0. \end{cases} \quad (18)$$

Here, X_i, Y_i, and Z_i are constant and depend on N, r, k, α, β, and λ. However, determining the conditions for their existence and finding their closed forms are generally a mathematically intractable problem as one will need to solve N simultaneous nonlinear PDEs. Moreover, due to the three separate conditions for each player, a complete analysis of the equilibrium may need to exhaustively include up to 3^N different market scenarios.

Nevertheless, some remarks can be said on the general behaviors for a particular player i.

1) $\Phi_i < 0$ implies $\pi < \alpha + 2\beta P_i^m + k\lambda(\partial V_i/\partial \pi)$. The market price π can be seen as the marginal revenue (MR), i.e., earnings from selling one extra unit of power. On the other hand, the right-hand side is the marginal cost (MC). As MR < MC, player i has no incentives to sell power.

2) Similarly, $\Phi_i > 0$ implies that MR > MC. That is, there are enough profits in the market for player i to output at maximum power.

3) $\Phi_i = 0$ implies that MR = MC, i.e., player i faces perfect competition and will have to select an output power that maximizes his profits. The optimal solution corresponds to the Markov NE strategy, which appears to be a linear feedback function of price π.

C. Solution in Oligopoly With Similar Constraints

In this section, we investigate a special case, i.e., a similar-constraint game where a complete characterization of the Markov feedback NE is obtainable. We assume that all players have similar constraints, i.e., $\widetilde{P_i^m} \equiv \widetilde{P^m}$, $\forall t, \forall i$. As a result, the game becomes symmetric and players' NE strategies are also symmetric with $P_i^{m*} = P^m$ and $V_i = V$, $\forall i$. The symmetry also reduces the game to three distinct market regions, depending on the value of $\pi(t)$.

1) Region 1—True Oligopoly: If the price $\pi(t)$ is such that the constraint $0 \leq P_i^m \leq \widetilde{P^m}$ is fulfilled, then all players maximize their profits by choosing the optimal strategy as the solution to $\Phi_i'(P_i^m) = 0$, where Φ_i' is the first order derivative of the maximand in (16) with respect to P_i^m. This scenario is therefore seen as the true-oligopoly case. Solution is obtained by applying Theorem 1 and solve the resulting PDEs.

Proposition 1: In region 1, the value function and its derivative have the following forms:

$$\frac{\partial V(\pi)}{\partial \pi} = X\pi - Y, \quad V(\pi) = \frac{1}{2}X\pi^2 - Y\pi + Z \quad (19a)$$

---

^{2}When dealing with the HJB equation and subsequent analysis, π is treated as a variable while the results should hold for all t; so π, $P_i^m(\pi)$ and $V_i(\pi)$ can be used instead of $\pi(t)$, $P_i^m(\pi(t))$, and $V_i(\pi(t))$.

This article has been accepted for inclusion in a future issue of this journal. Content is final as presented, with the exception of pagination.

LA *et al.*: POWER MANAGEMENT OF INTELLIGENT BUILDINGS FACILITATED BY SMART GRID: A MARKET APPROACH 7

where

$$X = \frac{(2\beta+N)k + \beta r - \sqrt{((2\beta+N)k+\beta r)^2 - (2N-\lambda)k^2\lambda}}{(2N-\lambda)k^2\lambda}$$

(19b)

$$Y = \frac{2\beta kaX + kN\alpha X - \alpha}{(2N-\lambda)k^2\lambda X - (2\beta+N)k - 2\beta r}$$

(19c)

$$Z = \frac{\alpha^2 + (2N-\lambda)k^2\lambda Y^2 - 2NkY\alpha - 4\beta kaY}{4\beta r}.$$

(19d)

The optimal strategy taken by each player is given by

$$P^{m*}(\pi) = \frac{1}{2\beta}[(1 - k\lambda X)\pi + (k\lambda Y - \alpha)].$$

(20)

The exact price trajectory $\pi(t)$ is given by

$$\pi(t) = \Gamma + C e^{-k\left[1 + \frac{N(1-k\lambda X)}{2\beta}\right]t}, \quad C = \text{const}$$

(21)

where Γ is the steady-state price in region 1, which equals

$$\Gamma = \frac{2\beta a + N(\alpha - k\lambda Y)}{2\beta + N(1 - k\lambda X)}.$$

(22)

Proof: Proof follows similar procedures as in [23]. ∎
In (21), C is found from initial condition $\pi(0)$ [e.g., $\pi(0) = \pi_0$ gives $C = \pi_0 - \Gamma$]. Moreover, $\lambda < 2N$ and (19b) imply that $X < (1/k\lambda)$ (details omitted). Consequently, the exponential term of (21) $\to 0$ and $\pi(t) \to$ stead-state price Γ as $t \to \infty$, provided that Γ lies within region 1. Γ is thus called the market equilibrium, the point of supply-demand balance. The boundaries for region 1 are prices where violations of $0 \le P_i^m \le \widetilde{P^m}$ start to occur. It can be shown that region 1 spans $\pi \in [\pi_1, \pi_2]$, where $\pi_1 = (\alpha - k\lambda Y)/(1 - k\lambda X)$ and $\pi_2 = (\alpha - k\lambda Y + 2\beta\widetilde{P_m})/(1 - k\lambda X)$.

2) Region 2—No Participation: In region 2, the optimal strategy occurs at the boundary $P^{m*} = 0$ for all players as the point where $\Phi_i'(P_i^m) = 0$ lies left of the interval $[0, \widetilde{P^m}]$, correspondingly $\pi < \pi_1$. In this region, players do not participate in the market due to inadequately low price which does not give them profits.

Proposition 2: In region 2, the players' equilibrium strategy is $P^{m*} = 0$ for all $\pi < \pi_1$. The steady-state price of this region is $\pi = a$, following a price trajectory:

$$\pi(t) = a + C e^{-kt}, \quad C = \text{const.}$$

(23)

The value function $V(\pi)$ in this region is given by

$$V(\pi) = V_1 \frac{(a - \pi_1)^{r/k}}{(a - \pi)^{r/k}}$$

(24)

where $V_1 = (1/2)X\pi_1^2 - Y\pi_1 + Z$.
Proof: Proof follows similar procedures as in [23]. ∎
Initial condition $\pi(0) = \pi_0$ gives $C = \pi_0 - a$.

3) Region 3—Output Saturation: In region 3, as opposed to region 2, equilibrium strategy occurs at the upper boundary, i.e., $P^{m*} = \widetilde{P^m}$ for all $\pi > \pi_2$. It is seen that as price level goes above the upper threshold value, all players will maximize their profits by outputting the maximum amount of power, i.e., their outputs become saturated.

Proposition 3: In region 3, the players' equilibrium strategy is $P^{m*} = \widetilde{P^m}$ for all $\pi > \pi_2$. The steady-state price of this region is $\pi = a - \lambda N\widetilde{P^m}$, following a price trajectory:

$$\pi(t) = a - \lambda N\widetilde{P^m} + C e^{-kt}, \quad C = \text{const.}$$

(25)

The value function $V(\pi)$ in this region is given by

$$V(\pi) = R\pi + S + (V_2 - R\pi_2 - S)\frac{\left(a - \lambda N\widetilde{P^m} - \pi_2\right)^{r/k}}{\left(a - \lambda N\widetilde{P^m} - \pi\right)^{r/k}}$$

(26)

where $V_2 = (1/2)X\pi_2^2 - Y\pi_2 + Z$, $R = (\widetilde{P^m}/r + k)$, and $S = (1/r)[k\widetilde{P_m}(a - \lambda N\widetilde{P^m})/(r + k) - \alpha\widetilde{P^m} - \beta\widetilde{P^{m2}}]$.
Proof: Proof follows similar procedures as in [23]. ∎
Initial condition $\pi(0) = \pi_0$ gives $C = \pi_0 - a + \lambda N\widetilde{P^m}$.
In summary, the overall Markov NE strategy is

$$P^{m*} = \begin{cases} \frac{1}{2\beta}[(1 - k\lambda X)\pi + (k\lambda Y - \alpha)] & \pi_1 \le \pi \le \pi_2 \\ 0 & \pi < \pi_1 \\ \widetilde{P^m} & \pi > \pi_2. \end{cases}$$

(27)

In summary, propositions 1–3 give a complete solution to the oligopoly competition in the seller market. We note in passing that the above analytical solution occurs in an ideal setting, where the buildings are able to control their strategies and price trajectory in continuous time via a feedback loop. In real systems, this is not feasible and the price movement should be approximated by discrete-time dynamics wherein price and traded power are constant during each time step. In the next section, we present our algorithm to implement this in practice and analyze convergence of the proposed method.

V. IMPLEMENTATION ALGORITHM

We describe our model for intelligent buildings in Section II, and the buyer and seller markets in Sections III and IV, respectively. This section puts everything together by introducing the implementation algorithm, shown in Algorithm 1. For each building as well as the broker who participate in the market, it also defines a protocol for interactions among the participants.

There are three major stages: 1) initialization (Stage I); 2) current period actions (Stage II); and 3) next period preparation (Stage III). During Stage I, each player estimates its current power stock (i.e., calculates $\widetilde{P_i^m}$ from $\widetilde{P_i^g}$, $\widetilde{P_i^l}$, and $\widetilde{P_i^s}$). Based on that value, it initiates to join an appropriate market by updating the broker of $\widetilde{P_i^m}$. In order to permit an oligopoly with similar constraints of $\widetilde{P_i^m}$, the broker decides an effective constraint $\widehat{P^m}$ and informs all players with power surplus ($i \in \mathcal{N}$) of this. Here, we let $\widehat{P^m} \triangleq \min_{i \in \mathcal{N}}\{\widetilde{P_i^m}\}$. In our simulation, we will justify this assumption. In Stage II, the N players with power surplus then play the game (14) to determine optimal P_i^{m*} to maximize profits. Players obtain the game solution as discussed in Section IV. The remaining $M - N$ players go to the buyer market and purchase their desired power via the broker. The broker adjusts the buyer market's price according to Section III. Once the current period ends, the algorithm enters Stage III where each player should update the remaining energy in its storage devices. The next period then begins

This article has been accepted for inclusion in a future issue of this journal. Content is final as presented, with the exception of pagination.

8   IEEE TRANSACTIONS ON SMART GRID

Algorithm 1 Detailed Implementation Steps

1: I. INITIALIZATION:
2: $\mathcal{N} \leftarrow \emptyset$
3: **for** player $i = 1 \rightarrow M$ **do**
4:     Estimate $\widetilde{P_i^g}, \widetilde{P_i^l}, \widetilde{P_i^s}$ and then $\widetilde{P_i^m}$
5:     **if** $\widetilde{P_i^m} > 0$ **then**   ▷ Power surplus
6:         Initiate to join the seller market, $\mathcal{N} \leftarrow \mathcal{N} \cup \{i\}$
7:     **else**   ▷ Power deficit
8:         Initiate to join the buyer market
9:     **end if**
10: **end for**
11: **for** broker **do**
12:     Set initial prices Π_0, π_0
13:     Inform all players $i \in \mathcal{N}$ of the effective constraint $\widehat{P^m}$
14: **end for**
15: II. CURRENT PERIOD:
16: **for** player $i \in \mathcal{N}$ **do**   ▷ Seller market
17:     Solve the game (14) according to Section IV
18:     Follow Alg. 2 for NE convergence   ▷ See Alg. 2
19:     Maintain $P_i^s(t)$ according to eq. (8)
20: **end for**
21: **for** player $i \notin \mathcal{N}$ **do**   ▷ Buyer market
22:     Buy the amount $\widetilde{P_i^m}$ from the broker
23: **end for**
24: **for** broker **do**
25:     Adjust π according to Alg. 2
26:     Adjust Π according to eq. (10)
27: **end for**
28: III. NEXT PERIOD:
29: **for** player $i = 1 \rightarrow M$ **do**
30:     Update $E_i^s(T)$ according to eq. (9)
31: **end for**
32: $\pi_0 \leftarrow$ current steady-state price
33: **Repeat** from Stage I

Algorithm 2 Discrete-Time Price Adjustment Method

Require: $t_0 = 0$, stepsize h
1: $n \leftarrow 0, \pi[t_0] \leftarrow \pi_0$ ▷ Initial price
2: **repeat**
3:     $n \leftarrow n + 1, t_{n+1} \leftarrow t_n + h$ ▷ Next time step
4:     Broker to update the price $\pi[t_{n+1}]$ according to

$$\pi[t_{n+1}] \leftarrow \pi[t_n] + h \times k(a - \pi[t_n] - \lambda \sum_{j=1}^{N} P_i^m[t_n]). \quad (28)$$

5:     **for** player $i \in \mathcal{N}$ **do**
6:         $P_i^m[t_{n+1}] \leftarrow P_i^{m*}(\pi[t_{n+1}])$ according to (27)
7:     **end for**
8: **until** $t_n > T$

---

similarly to the previous one, i.e., starting from Stage I, with the initial market price set to the previous steady-state value.

At lines 18 and 25 of Algorithm 1, players and broker execute another algorithm to converge to the NE. This method, Algorithm 2, is introduced because theoretically, players and broker must update power and price instantaneously in a feedback loop which may not be feasible in practice. Algorithm 2 hence allows them to adjust power and price in a feasible discrete-time basis, i.e., periodic updates at a predetermined short interval of a stepsize h. At each time step, the broker updates the price $\pi[t_{n+1}]$ based on its previous value $\pi[t_n]$ and the previous supplied power $P_i^m[t_n]$, following (28). For each player, $P_i^m[t_{n+1}]$ is updated according to (27) which gives the optimal strategy. The method continues until the current period has elapsed, i.e., $t_n > T$.

Convergence of Algorithm 2 hinges upon the stepsize h. It can be proven that the algorithm will converge as long as h does not exceed a maximum amount and stated as follows.

TABLE I
PARAMETER SETTINGS

Parameters	Values
Number of players, M	8
Interval, T (PV system)	30 min
Interval, T (wind turbine system)	5 min
Solar conversion efficiency, η_{PV}	0.157
Area of PV cells, A_{PV}	80 m^2
Outside air temperature, T_{air}	30 ^{o}C
Rated wind turbine power, P_{WT}	50 kW
Rated wind turbine wind speed, v_r	12 m/s
Cut-in wind turbine wind speed, v_{in}	3 m/s
Cut-out wind turbine wind speed, v_{out}	30 m/s
Storage charge/discharge efficiency, η	0.9
Initial storage capacity, C_0	2 kWh
Initial stored energy, $E_i^s(0)$	1 kWh
Storage capacity loss coefficient, ϵ	3×10^{-4}
Maximum charging rate, P_{max}^s	5 kW
Initial prices, Π_0 and π_0	9 \$/kW
Parameters specific to market:	
a	17 \$/kW
λ	1 \$/(kW)^2
k	0.5
r	0.1
α	1.5 \$/kW
β	0.5 \$/(kW)^2
γ	10/7

Proposition 4: Algorithm 2 will converge as long as a stepsize h is chosen such that

$$h < h_{max} = \frac{2}{k\left[1 + \dfrac{\lambda N(1 - k\lambda X)}{2\beta}\right]} \quad (29)$$

.

Proof: Omitted for brevity.   ∎

VI. SIMULATION RESULTS

Extensive computer simulations on various aspects of the proposed model are carried out using MATLAB. We select the key parameters according to Table I. Systems using either PV or wind turbine generation can be considered. An interval of $T = 30$ (min) is assumed for PV generation [18], whereas $T = 5$ (min) for wind generation [9]. Note that for convenience, we simulated the two cases separately but a hybrid system can easily be implemented using $T = 5$ (min) as the interval. The solar efficiency value η_{PV} follows that of [35]. The parameters pertaining to the storage devices (C_0, P_{max}^s, η, ϵ, and so on) are adapted from Li-ion batteries used in actual microgrids [5], [35]. In addition, in (10), we set $\gamma = 10/7$ which corresponds to a price elasticity of demand $1/\gamma = 0.7$. This value agrees with a recent empirical study of the Singapore energy market [33], which reported a price elasticity in the range from 0.35 to 1.07. Although the settings may not represent perfectly an actual energy market, the examples could be useful to illustrate the model's behaviors.

A. Convergence of the Oligopoly

We first verify our analysis of the oligopoly game for the seller market with a numerical example for a single period among a few buildings with PV generation. We also assume that in this example, there are $N = 4$ sellers; solar irradiance

This article has been accepted for inclusion in a future issue of this journal. Content is final as presented, with the exception of pagination.

LA *et al.*: POWER MANAGEMENT OF INTELLIGENT BUILDINGS FACILITATED BY SMART GRID: A MARKET APPROACH
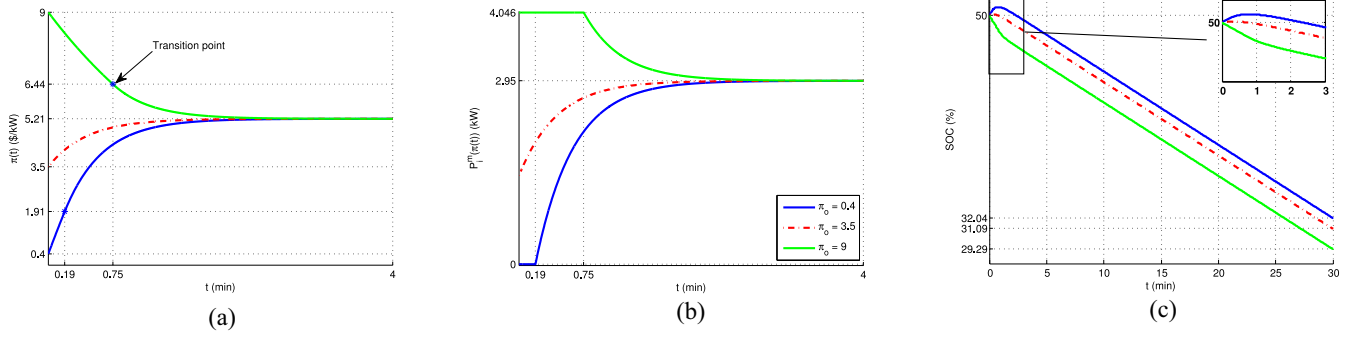
9

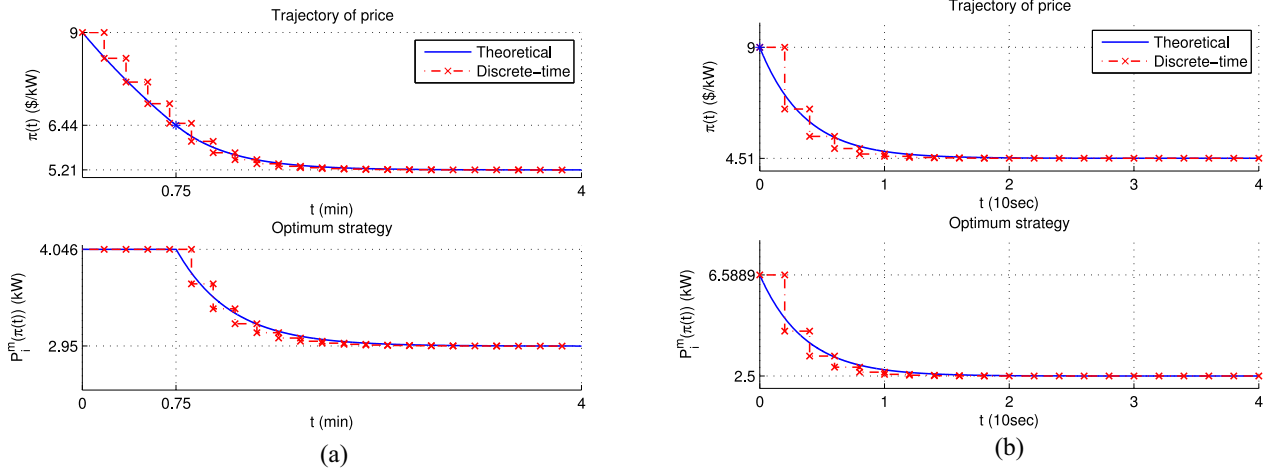Fig. 3. Values over one interval for (a) price, (b) strategy, and (c) SoC.

Fig. 4. Convergence of the discrete-time method with (a) PV generation and (b) wind generation.

forecast is $\widetilde{I_{\mathrm{PV},i}} = 1$ kW/m^2; and $\widetilde{P_i^l} = 9$ kW, $\forall i$. Equation (7) thus leads to a power surplus of $\widetilde{P_i^m} = 4.046$ kW available for trading. Fig. 3 plots the results for (a) the price trajectory and (b) the players' optimal power output as well as (c) the storage device's real-time SoC. Clearly, the price $\pi(t)$ and the strategy P_i^m quickly approaches steady-state values. For illustration, Fig. 3(a) and (b) only displays up to $t = 4$ min when NE convergence has already occurred. Thus, the total interval $T = 30$ min is sufficiently large to justify our infinite horizon assumption. Moreover, while three different initial prices (0.4, 3.5, and 9) are examined, the equilibrium price is unique and independent of π_0, since the trajectory equation is linear in π which allows the system to admit a unique steady-state price $\Gamma = 5.21$ in region 1. Here, the regions are defined at $\pi_1 = 1.91$ and $\pi_2 = 6.44$. Different values of π_0 result in different starting regions as seen in Fig. 3(b). Along the trajectory, when $\pi(t)$ reaches π_1 or π_2, a transition from one region to another occurs, evident in the shapes of P_i^m at $t = 0.19$ and $t = 0.75$. The transition mechanism is discussed in [23] and not repeated here.

In this context, we define SoC in Fig. 3(c) as the percentage of current stored energy $E_i^s(t)$ over maximum capacity $C_i^s(t)$. Note that the value of SoC directly depends on the behavior of $P_i^s(t)$ whose shape, following (8), mirrors that of P_i^m in Fig. 3(b). Take the case of $\pi_0 = 0.4$ for example. Fig. 3(c) shows that the SoC first experiences a nonlinear increase, then starts to decrease and its slope is asymptotically

constant toward the steady state. Here, the original increase in SoC is due to the starting value of $P_i^s(0)$ which is computed to be 2.25 kW, i.e., battery charging. Then, after $t = 0.19$, $P_i^m(t)$ starts to increase nonlinearly as seen in Fig. 3(b) and hence, $P_i^s(t) = \widetilde{P_i^g} - \widetilde{P_i^l} - P_i^m(t)$ decreases correspondingly. At some point before $t = 0.82$, $P_i^s(t)$ should cross 0 and become negative, which means the battery starts to discharge and SoC decreases. Eventually, as $P_i^m(t)$ converges to its steady-state value, so does $P_i^s(t)$ to a value of about -0.702 kW. This corresponds to the slope of the SoC at the steady state as shown in Fig. 3(c). Similar observations can be seen for the other π_0. We note also that different values of π_0 slightly affect the final SoC values at the end of the interval, as smaller π_0 leads to less power traded and more remaining in the battery, hence a higher SoC.

This example is given for a system with PV generation. However, the results equally apply to the case of wind energy.

B. Evaluation of the Discrete-Time Algorithm

Next, we validate Algorithm 2. Using the previous settings as well as $\pi_0 = 9$, the discrete-time price and traded power obtained under Algorithm 2 are shown in Fig. 4(a), together with their theoretical counterparts from $t = 0$ to $t = 4$ min. The maximum stepsize according to Proposition 4 is $h_{\max} \approx 0.8739$ (min). The chosen stepsize is $h = 0.2 h_{\max}$. As predicted, a properly chosen h ensures Algorithm 2 timely convergence within 4 min. This corresponds to the case of
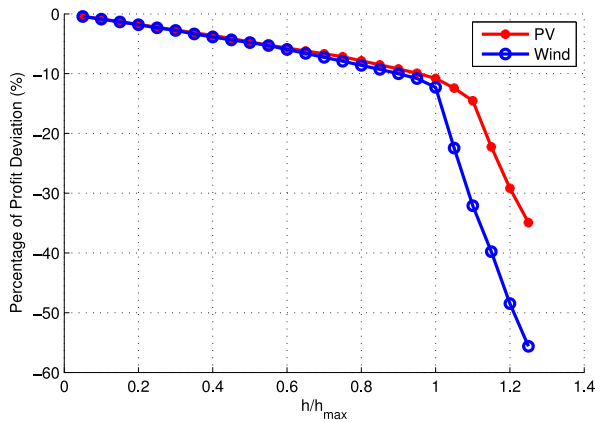
This article has been accepted for inclusion in a future issue of this journal. Content is final as presented, with the exception of pagination.

10

IEEE TRANSACTIONS ON SMART GRID

Fig. 5.   Profit deviation from ideal value versus stepsize.

Fig. 6.   Steady state values for (a) price and (b) strategy, against different numbers of players.

PV generation. We are also interested in the convergence for wind generation under a shorter interval of $T = 5$ min. Consequently, we adopted a different unit of 10 s for the time variable t and applied the algorithm accordingly. In the simulation for wind generation, we have assumed similar settings as in Table I except for $T = 30 \times 10$ s or 5 min, $E_i^s(0) = 0.25$ kWh, and wind speed $\widetilde{v}_i = 5.5$ m/s. Convergence plots are then obtained as in Fig. 4(b), which shows a similar behavior. The corresponding maximum stepsize is computed to be $h_{\max} \approx 7.1919$ s and we select $h = 2$ s. The algorithm then converges within 30 s.

Discrepancy between the discrete and theoretical solutions, especially in the transient state can affect the player's aggregate profit. We study such impacts under varying stepsizes. Fig. 5 plots the percentage of profit deviation, $\Delta J = (J^* - J_d)/J^* \times 100\%$ where J_d and J^* respectively are the discrete-time and theoretical profits from (13), against the ratio $h/h_{\max}$. Both PV and wind generation are considered; however, there is not any significant difference between them when $h < h_{\max}$. As predicted, when $h/h_{\max} > 1$, ΔJ diverges drastically which further confirms our analysis. The divergence $\to \infty$ as $T \to \infty$. Meanwhile, ΔJ grows (nonlinearly but the slope can be linearly approximated) as h increases within its feasible range, as larger h leads to slower convergence and bigger deviation. Notice $\Delta J < 0$, $\forall h$, since any trajectories other than the theoretically maximum profit J^* will result in lower profit. The profit loss is within 10% of J^*. There is an accuracy and computation tradeoff, as a smaller h gives slightly more profit but with more computations.

C. Impacts of the Number of Oligopolists

The impacts of the number of players N in the dynamic oligopoly on the market behaviors, especially the steady-state values, are also investigated. Also based on the previous settings, we obtain various steady-state values of the game for various N and plot the results in Fig. 6. It can be observed that in this example, except for $N = 2$, where the game ends in region 3, for any other N, the game ends in region 1. Thus, the steady state values of $\pi(t)$ and P_i^{m*} are Γ and $P^{m*}(\Gamma)$, respectively. Both are seen to drop as N grows larger. Economically, it can be explained that more competitors increase the aggregate supplies which brings down the equilibrium price. Also,
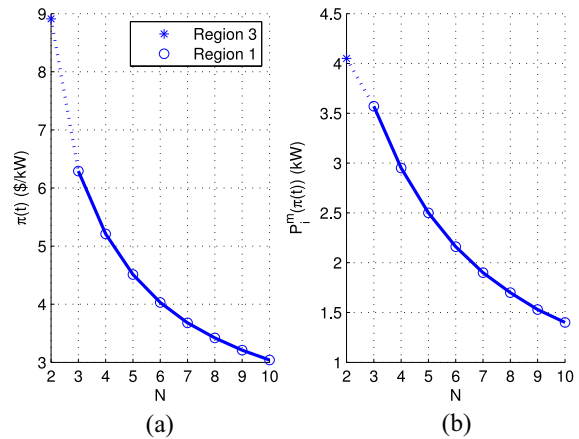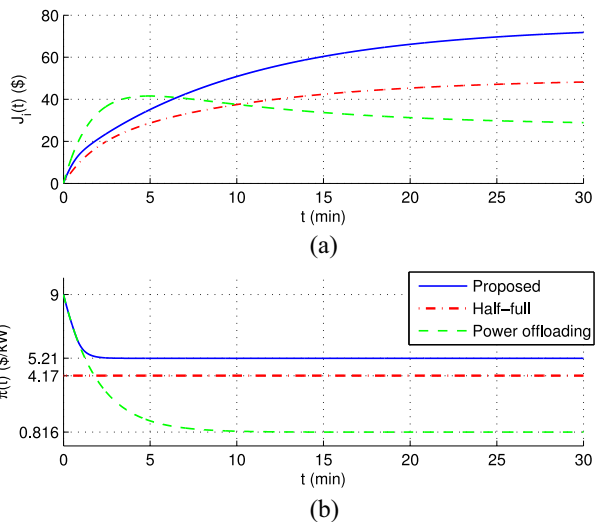

Fig. 7.   Comparison of the proposed scheme and power offloading scheme for (a) accumulated profit and (b) price.

each player gets a smaller share of the market; hence, their traded powers also drop.[3]

D. Comparison of Accumulated Profit

For a better assessment of the proposed scheme, we compare it to other schemes in terms of the aggregate profit up to time t. This comparison metric is $J_i(t) = \int_0^t e^{-r\tau}\{P_i^m(\tau)\pi(\tau) - \alpha P_i^m(\tau) - \beta[P_i^m(\tau)]^2\}d\tau$. Two alternative schemes are considered: 1) half-full and 2) power-offloading.

The first scheme considered here is a deterministic strategy: a building with myopic knowledge sells part of the available power while maintaining the rest for some flexibility, often at half capacity, i.e., "half-full." This method has been considered as a reference point in [15] and [34]. In this scheme, we assume no dynamic pricing and competition takes place and price is set at its region 1s value of π corresponding to $P_i^m = \widetilde{P}_i^m/2$ using (20).

[3]Mathematically, one can prove that as $N \to \infty$, $\Gamma \to \alpha$, and $P^{m*}(\Gamma) \to 0$ (assuming final equilibrium in region 1).

This article has been accepted for inclusion in a future issue of this journal. Content is final as presented, with the exception of pagination.

LA *et al.*: POWER MANAGEMENT OF INTELLIGENT BUILDINGS FACILITATED BY SMART GRID: A MARKET APPROACH 11

TABLE II
VALUES OF $\widetilde{P_i^m}$ AND STEADY-STATE OUTPUT POWER IN kW

	Period 1	Period 2	Period 3	Period 4
Player 1	6.025	-3.047	**4.915**	4.822
Player 2	**5.616**	5.745	6.678	-4.631
Player 3	6.617	7.382	-3.388	-7.035
Player 4	-4.793	-6.865	-6.888	-7.300
Player 5	-3.790	5.108	-4.572	5.805
Player 6	-4.194	5.142	-4.714	4.119
Player 7	7.263	-3.853	-5.728	**3.464**
Player 8	-6.432	**4.509**	5.742	-5.943
P_{std}^m (kW)	2.948	2.497	3.571	2.948

The second scheme, power-offloading, is when buildings do not utilize storage devices and sell all of their surplus power. For a fair comparison, power-offloading also follows the same pricing dynamic (12) as the proposed method. Without storage, the quadratic cost in $J_i(t)$ which accounts for battery penalty is removed, i.e., $\beta = 0$ for power-offloading.

Using the previous settings, Fig. 7 plots $J_i(t)$ and the price $\pi(t)$ over one interval $[0, T]$ for the three schemes. We see that against the deterministic half-full scheme, our proposed method, which employs dynamic pricing to allow players to adjust to toward their optimal power levels, is consistently generating better profit. For power-offloading, it initially delivers higher profit at the beginning, since it is helped by the high starting price π_0 and the absence of the second-order cost term. However, in the long run when price stabilizes, the proposed scheme maximizes profit while power-offloading sees a profit decline. As players always sell maximum power, more supply leads to decreasing steady-state price (0.816 $/kW, which is region 3 s steady state). This price cannot cover the cost rate $\alpha = 1.5$ $/kW; as such, player incurs a negative marginal profit and $J_i(t)$ decreases.

E. System Behaviors Over Multiple Intervals

In the next study, we examine the system's operations over multiple periods, using parameters in Table I. Again, we simulated a system with PV generation but the method can be applied to wind generation without loss of generality. For simulation purposes, at the start of each interval, a player has a 50:50 chance of either in surplus or deficit. For power surplus, we assume players experience solar irradiance of $\widetilde{I_i} \sim \text{Unif}(0.9, 1.0)$ kW/m^2; while their loads follow $\widetilde{P_i^l} \sim \text{Unif}(8, 9)$ kW. For power deficit, $\widetilde{I_i} \sim \text{Unif}(0.45, 0.65)$ kW/m^2; and $\widetilde{P_i^l} \sim \text{Unif}(12, 14)$ kW. These values have been matched to real-time data [24] of the practical loads and generated power from renewable sources. Table II displays for all players their power stock $\widetilde{P_i^m}$ for 4 consecutive periods. Those with negative $\widetilde{P_i^m}$ buy this amount from the market, while others play the oligopoly game. The common constraint $\widehat{P^m}$ is decided (boldface, Table II). The last row gives the steady-state strategy P_{std}^m. Take period 1 for example. The 4 players with power surplus (1, 2, 3, and 7) have $\widetilde{P_i^m} = 6.025$, 5.616, 6.617, and 7.263 kW, respectively. Since these values are closely spread, we could reasonably select $\widehat{P^m} = 5.616$ kW as a common constraint. Furthermore, at the steady state, $P_{std}^m = P^{m*}(\Gamma) = 2.948$ kW which is not at maximum level $\widehat{P^m}$. From (20) and (22), we know that $P^{m*}(\Gamma)$ does
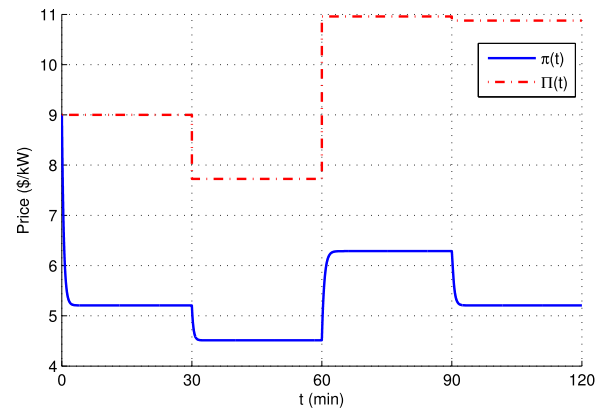

Fig. 8. Movement of market prices over multiple periods.

not depend on $\widehat{P^m}$. In the other periods, the values of $\widetilde{P_i^m}$ are also closed enough (except period 2 where $\widetilde{P_i^m}$ varies remarkably but $P_{std}^m = 2.497$ kW still lies in region 1 and independent of $\widehat{P^m}$). Thus, our use of $\widehat{P^m}$ is partly justified here.

Lastly, Fig. 8 shows both the seller market price $\pi(t)$ and the buyer market price $\Pi(t)$ over four simulated periods. In all periods, $\pi(t)$ shortly reaches steady states. Note also that these steady-states (at Γ) vary inversely with the number of players N. For instance, $N = 4$ and $\Gamma = 5.21$ $/kW in period 1. In period 2, $N = 5$ and Γ drops to 4.51 $/kW, and so on. This observation on N and steady-state price is similar to those in [15] and [23]. On the other hand, Π varies independently from π but reflects the buyer market trend across periods, according to (10). Specifically, from periods 1 to 2, the market sees a decline as the net demand $Q_1 = 19.209$ kW decreases to $Q_2 = 13.765$ kW. As such, the price also drops from $\Pi_1 = 9$ to $\Pi_2 = 7.72$ $/kW. Similar trends are seen in other periods.

VII. CONCLUSION

In this paper, we develop a model to account for the operation of generator, storage, and load for an intelligent building, as well as for multiple buildings in a cluster. An energy market enables buildings to buy power when in deficit, and sell power via a broker when in surplus. Subsequently, we devise dynamic pricing schemes for both buyer market and especially seller market, where an oligopoly differential game is set up. The mathematical analysis for this game is presented. We also propose a practical price and strategy update scheme that works in real time. Simulation studies are carried out to verify our model and analysis. The proposed game optimizes the profits accumulated over time, compared to other power management schemes.

REFERENCES

[1] Singapore National Environment Agency. (2014). *E2 Singapore*. [Online]. Available: http://app.e2singapore.gov.sg/DATA/0/docs/Booklet/E2S%20Publication.pdf

[2] U.S. Department of Energy. (2011). *Buildings Energy Data Book*. [Online]. Available: http://buildingsdatabook.eren.doe.gov/

[3] R. H. Lasseter, "Smart distribution: Coupled microgrids," *Proc. IEEE*, vol. 99, no. 6, pp. 1074–1082, Jun. 2011.

[4] B. Kroposki *et al.*, "Making microgrids work," *IEEE Power Energy Mag.*, vol. 6, no. 3, pp. 40–53, May/Jun. 2008.

[5] M. Marzband, A. Sumper, A. Ruiz-Álvarez, J. L. Domínguez-García, and B. Tomoiagă, "Experimental evaluation of a real time energy management system for stand-alone microgrids in day-ahead markets," *Appl. Energy*, vol. 106, pp. 365–376, Jun. 2013.

[6] G. T. Heydt *et al.*, "Pricing and control in the next generation power distribution system," *IEEE Trans. Smart Grid*, vol. 3, no. 2, pp. 907–914, Jun. 2012.

[7] Y. Ding *et al.*, "Real-time market concept architecture for EcoGrid EU—A prototype for European smart grids," *IEEE Trans. Smart Grid*, vol. 4, no. 4, pp. 2006–2016, Dec. 2013.

[8] D. T. Nguyen and L. B. Le, "Optimal bidding strategy for microgrids considering renewable energy and building thermal dynamics," *IEEE Trans. Smart Grid*, vol. 5, no. 4, pp. 1608–1620, Jul. 2014.

[9] Z. Ding, Y. Guo, D. Wu, and Y. Fang, "A market based scheme to integrate distributed wind energy," *IEEE Trans. Smart Grid*, vol. 4, no. 2, pp. 976–984, Jun. 2013.

[10] A. Damiano, G. Gatto, I. Marongiu, M. Porru, and A. Serpi, "Real-time control strategy of energy storage systems for renewable energy sources exploitation," *IEEE Trans. Sustain. Energy*, vol. 5, no. 2, pp. 567–576, Apr. 2014.

[11] W. Lee, L. Xiang, R. Schober, and V. W. S. Wong, "Direct electricity trading in smart grid: A coalitional game analysis," *IEEE J. Sel. Areas Commun.*, vol. 32, no. 7, pp. 1398–1411, Jul. 2014.

[12] X. Guan, Z. Xu, and Q.-S. Jia, "Energy-efficient buildings facilitated by microgrid," *IEEE Trans. Smart Grid*, vol. 1, no. 3, pp. 243–252, Dec. 2010.

[13] Z. Zhou, X. Zhang, and Y. M. Lee, "An inventory control and pricing model for smart building load management," in *Proc. IEEE/PES Innov. Smart Grid Technol. Conf. (ISGT)*, Washington, DC, USA, 2014, pp. 1–5.

[14] X. Fang, S. Misra, G. Xue, and D. Yang, "Smart grid—The new and improved power grid: A survey," *IEEE Commun. Surveys Tuts.*, vol. 14, no. 4, pp. 944–980, Oct./Dec. 2012.

[15] Q. D. La, Y. W. E. Chan, and B.-H. Soong, "Dynamic market for distributed energy resources in the smart grid," in *Proc. IEEE CCNC*, Las Vegas, NV, USA, Jan. 2014, pp. 38–43.

[16] Y. Ru, J. Kleissl, and S. Martinez, "Storage size determination for grid-connected photovoltaic systems," *IEEE Trans. Sustain. Energy*, vol. 4, no. 1, pp. 68–81, Jan. 2013.

[17] C. W. Potter, A. Archambault, and K. Westrick, "Building a smarter smart grid through better renewable energy information," in *Proc. IEEE/PES PSCE*, Seattle, WA, USA, 2009, pp. 1–5.

[18] H. Kanchev, D. Lu, F. Colas, V. Lazarov, and B. Francois, "Energy management and operational planning of a microgrid with a PV-based active generator for smart grid applications," *IEEE Trans. Ind. Electron.*, vol. 58, no. 10, pp. 4583–4592, Oct. 2011.

[19] Singapore Energy Market Authority. (2014). *Contestable Consumers*. [Online]. Available: http://www.ema.gov.sg/Non_Residential_Contestable_Consumers.aspx

[20] M. Sewalt and C. De Jong, "Negative prices in electricity market," *Commod. Now*, pp. 74–77, Jun. 2003.

[21] E. Dockner, S. Jørgensen, N. V. Long, and G. Sorger, *Differential Games in Economics and Management Science*. Cambridge, U.K.: Cambridge Univ. Press, 2000.

[22] D. W. K. Yeung and L. A. Petrosyan, *Cooperative Stochastic Differential Games*. New York, NY, USA: Springer, 2006.

[23] Q. D. La, Y. H. Chew, and B.-H. Soong, "Oligopolistic spectrum allocation game via market competition under spectrum broker," *Comput. Netw.*, vol. 70, pp. 225–239, Sep. 2014.

[24] Pennsylvania-New Jersey-Maryland (PJM) Interconnection LLC. (Jul. 7, 2015). *Energy Market*. [Online]. Available: http://www.pjm.com/markets-and-operations/energy.aspx

[25] F. Wen and A. K. David, "Optimal bidding strategies and modeling of imperfect information among competitive generators," *IEEE Trans. Power Syst.*, vol. 16, no. 1, pp. 15–21, Feb. 2001.

[26] A. R. Kian and J. B. Cruz, Jr., "Bidding strategies in dynamic electricity markets," *Decis. Support Syst.*, vol. 40, nos. 3–4, pp. 543–551, Oct. 2005.

[27] R. Lau *et al.*, "Strategy and modeling for building DR optimization," in *Proc. IEEE SmartGridComm*, Brussels, Belgium, 2011, pp. 381–386.

[28] B. Jiang and Y. Fei, "Smart home in smart microgrid: A cost-effective energy ecosystem with intelligent hierarchical agents," *IEEE Trans. Smart Grid*, vol. 6, no. 1, pp. 3–13, Jan. 2015.

[29] S. Lee, B. Kwon, and S. Lee, "Joint energy management system of electric supply and demand in houses and buildings," *IEEE Trans. Power Syst.*, vol. 29, no. 6, pp. 2804–2812, Nov. 2014.

[30] H. T. Nguyen and L. B. Le, "Optimal energy management for building microgrid with constrained renewable energy utilization," in *Proc. IEEE SmartGridComm*, Venice, Italy, 2014, pp. 133–138.

[31] A. Mishra, D. Irwin, P. Shenoy, J. Kurose, and T. Zhu, "GreenCharge: Managing renewable energy in smart buildings," *IEEE J. Sel. Areas Commun.*, vol. 31, no. 7, pp. 1281–1293, Jul. 2013.

[32] A. A. Sánchez de la Nieta, J. Contreras, J. I. Muñoz, and M. O'Malley, "Modeling the impact of a wind power producer as a price-maker," *IEEE Trans. Power Syst.*, vol. 29, no. 6, pp. 2723–2732, Nov. 2014.

[33] H. Phoumin and S. Kimura, "Analysis on price elasticity of energy demand in East Asia: Empirical evidence and policy implications for ASEAN and East Asia," Econ. Res. Inst. ASEAN East Asia (ERIA), Jakarta, Indonesia, Tech. Rep. DP-2014-05, 2014.

[34] P. A. Coppin, "Using intelligent storage to smooth wind energy generation," in *Proc. Elect. Energy Stor. Appl. Technol. Conf.*, San Francisco, CA, USA, Sep. 2007.

[35] S. X. Chen, H. B. Gooi, and M. Q. Wang, "Sizing of energy storage for microgrids," *IEEE Trans. Smart Grid*, vol. 3, no. 1, pp. 142–151, Mar. 2012.

[36] J. Bushnell, "Oligopoly equilibria in electricity contract markets," *J. Regul. Econ.*, vol. 32, no. 3, pp. 225–245, Dec. 2007.

[37] Y. Chen and B. F. Hobbs, "An oligopolistic power market model with tradable NO_x permits," *IEEE Trans. Power Syst.*, vol. 20, no. 1, pp. 119–129, Feb. 2005.

Quang Duy La (S'09–M'14) received the B.Eng. degree (with first-class Hons.) in electrical and electronic engineering and the Ph.D. degree in electrical and electronic engineering under the Nanyang Presidents Research Scholarship from Nanyang Technological University, Singapore, in 2008 and 2013, respectively.

He is currently a Postdoctoral Research Fellow with Temasek Laboratories, Singapore University of Technology and Design, Singapore. He has participated in research projects on radio resource allocation, smart grid, wireless body area networks, and network security. His current research interests lie in game theory, optimization techniques, and distributed algorithms for next generation communications systems.

Yiu Wing Edwin Chan (S'12) received the B.Eng. degree (with first class Hons.) in electrical and electronic engineering from the University of Auckland, Auckland, New Zealand, in 2001. He is currently pursuing the Ph.D. degree with Nanyang Technological University (NTU), Singapore.

As a Research Engineer at NTU, he joined the Singapore-Berkeley Building Efficiency and Sustainability in the Tropics Program of the Berkeley Education Alliance for Research in Singapore, and has been participating in research projects on intelligent lighting system, building automation, and smart grid. His current research interests include localization, wireless sensor networks, and wireless communications.

Boon-Hee Soong (M'90–SM'04) received the B.Eng. (Hons.) degree in electrical and electronic engineering from the University of Auckland, Auckland, New Zealand, in 1984, and the Ph.D. degree from the University of Newcastle, Newcastle, NSW, Australia, in 1990.

He is currently an Associate Professor with the School of Electrical and Electronic Engineering, Nanyang Technological University, Singapore. His current research interests include network performance analysis, and mobile and wireless communications.

Dr. Soong was a recipient of the Commonwealth Fellowship Award in 1999 and the Tan Chin Tuan Fellowship Award in 2004.